Contemporary Mathematics
http://ojs.wiserpub.com/index.php/CM/

Research Article

An Analytical and Numerical Approach to Solve the Tsunami Wave Propagation Equation

Juhi Kesarwani[1*], Abhijit Majumder[1], Ishita Sharma[1], Ashish Kumar Kesarwany[2]

[1]Department of Mathematics, Lovely Professional University, Phagwara-144411, Punjab, India
[2]Department of Mathematics, Indian Institute of Technology, Guwahati-781039, Assam, India
E-mail: juhi.28923@lpu.co.in

Received: 6 April 2023; **Revised:** 23 May 2023; **Accepted:** 9 June 2023

Abstract: We study the mathematical model of tsunami wave propagation (TWP) along the coastline of an ocean. The described model is represented by a system of non-linear partial differential equations. In this study, we employ two different techniques: one is the Adomian decomposition method (ADM, which is an analytical approach), and another is the finite difference method (FDM, which is a numerical approach) to obtain the solution for the proposed TWP model successfully. The solutions gained are numerically represented in graphs and tables. The validity of the solutions is investigated by comparing this proposed method with the fractional reduced differential transform method (FRDTM). The novelty of this paper is that we have demonstrated that the numerical method (FDM) better approximates the solution of our partial differential equation than the analytical method (ADM), and this has not been explored before in any other works. We examine the velocity and height of the coastline of an ocean from the tsunami wave equation using numerical and analytical techniques. MATLAB and MAPLE are used to obtain numerical and graphical representations.

Keywords**:** tsunami model, FDM, ADM, non-linear partial differential equation

1. Introduction

A tsunami is a sequence of large-wavelength ocean waves caused by a saltwater disturbance close to the coast. Most tsunamis are brought on by changes in the seabed's earthen crust, such as seabed earthquakes, landslides, or volcanic eruptions that result in elevated water levels over vast areas [1]. Although the sources that cause tsunamis are considered point sources, the tsunami waves produced can be highly devastating locally. The energy of the waves can ravage coasts, inflicting property damage and fatalities. The speed of the tsunami is governed by the water depth [2]. A tsunami occurrence can be divided into three phases: generation, propagation, inundation, and landfall [3]. Since each tsunami is unique and no single process can explain all tsunamis, the generation stage is the most complex and challenging to examine. Again, no single scenario can adequately illustrate all affected places because the inundation stage varies for all affected areas. Although thorough numerical models are available in the literature, the propagation stage is the only one that can be handled by straightforward theory and analysis and spans the largest region [4]. Many researchers have discussed this type of problem in a different way (see, for example [5-18]). Many scholars have studied the phenomenon of tsunami waves from various angles and perspectives [19, 20]. But every time, it is not possible to find an exact solution to a problem. Defining the analytical solution to the tsunami wave propagation (TWP) equation is

DOI: https://doi.org/10.37256/cm.6120252793

not an easy task because of some limitations. Even though some authors [21-28] have defined the solution of the non-linear TWP equation by different methods, Younesian et al. [29] have obtained an analytical solution for non-linear wave propagation in shallow media using the variational iteration method. Karunakar and Chakraverty [30] have studied the homotopy perturbation method for predicting TWP with crisp and uncertain parameters. Recently, researchers [31, 32] have applied the Sine Gordon expansion method, which transforms the shallow water partial differential equations (PDEs) to ordinary differential equations (ODEs), and the solutions are obtained in a complex manner. In contrast, in this work, the authors have employed the Adomian decomposition method (ADM), which does not involve linearization and gives real solutions.

The originality of this research lies in the fact that we show that the numerical approach (finite difference method; FDM) approximates the solution of the non-linear TWP equation more accurately than the analytical method (ADM), which has never been investigated in prior works. We use numerical and analytical methods to assess the velocity and height of an ocean's coastline as derived from the tsunami wave equation.

TWP model with a system of non-linear PDE [19] is defined as

$$\partial_t \phi + \phi \partial_x \phi + g \partial_x \psi = 0, \tag{1}$$

$$\partial_t \psi + \partial_x \left[\phi \left(d' + \psi \right) \right] = 0, \tag{2}$$

with some initial condition

$$\phi(x, 0) = H\sqrt{\frac{g}{d}} \operatorname{sech}^2\left(\sqrt{\frac{3H}{4d^3}}x\right), \ \psi(x, 0) = H \operatorname{sech}^2\left(\sqrt{\frac{3H}{4d^3}}x\right). \tag{3}$$

Here, the tsunami velocity is denoted by $\phi(x, t)$, the wave amplification is denoted by $\psi(x, t)$ the ocean depth near the coast is denoted by d' the gravitational acceleration is denoted by g, and H denotes the original wave amplification.

2. Review of the ADM

This section discusses a brief analysis of the ADM. ADM [33] is an analytical method to solve linear and non-linear PDEs. Take into account the set of partial differential equations as

$$\begin{aligned} &\partial_t \phi + R_1(\phi, \psi) + N_1(\phi, \psi) = \mathcal{G}_1, \\ &\partial_t \phi + R_2(\phi, \psi) + N_2(\phi, \psi) = \mathcal{G}_2, \end{aligned} \tag{4}$$

with initial conditions

$$\phi(x, 0) = \mathcal{F}_1(x), \ \psi(x, 0) = \mathcal{F}_2(x). \tag{5}$$

where ∂_t is defined as the differential operator, R_1 and R_2 are defined as linear operator, N_1 and N_2 are defined as non-linear operators, $\mathcal{G}_1$ and $\mathcal{G}_2$ are defined as non-homogeneous terms.

Taking the inverse of both sides of equation (4) and using initial conditions (5), we get

$$\int \partial_t \phi dt + \int R_1(\phi, \psi) dt + \int N_1(\phi, \psi) dt = \int \mathcal{G}_1 dt, \ \int \partial_t \psi dt + \int R_2(\phi, \psi) dt + \int N_2(\phi, \psi) dt = \int \mathcal{G}_2 dt \tag{6}$$

After simplification, it gives

$$\phi = \mathcal{F}_1(x) + \int g_1 dt - \int R_1(\phi, \psi) dt - \int N_1(\phi, \psi) dt, \ \ \psi = \mathcal{F}_2(x) + \int g_2 dt - \int R_2(\phi, \psi) dt - \int N_2(\phi, \psi) dt. \tag{7}$$

The ADM decomposes both functions $\phi(x, t)$ and $\psi(x, t)$ as an infinite series

$$\phi(x, t) = \sum_{n=0}^{\infty} \phi_n(x, t), \ \ \psi(x, t) = \sum_{n=0}^{\infty} \psi_n(x, t). \tag{8}$$

And non-linear terms $N_1(\phi, \psi)$ and $N_2(\phi, \psi)$ can be represented by an Adomian polynomials as

$$N_1(\phi, \psi) = \sum_{n=0}^{\infty} \mathbb{A}_n, \ N_2(\phi, \psi) = \sum_{n=0}^{\infty} \mathbb{B}_n.$$

For all types of non-linearity, the Adomian polynomials can be produced. The following relations determine them:

$$\mathbb{A}_n = \frac{1}{n!}\left[\frac{d^n}{d\lambda^n}\left[N_1 \sum_{i=0}^{\infty}\left(\lambda^i \phi_i\right)\right]\right]_{\lambda=0},$$

$$\mathbb{B}_n = \frac{1}{n!}\left[\frac{d^n}{d\lambda^n}\left[N_2 \sum_{i=0}^{\infty}\left(\lambda^i \psi_i\right)\right]\right]_{\lambda=0} \tag{9}$$

Substituting equations (8) and (9) into equation (7), it gives

$$\sum_{n=0}^{\infty} \phi_n(x, t) = \mathcal{F}_1(x) + \int \mathcal{G}_1 dt - \int\left(R_1\left(\left[\sum_{n=0}^{\infty} \phi_n\right], \left[\sum_{n=0}^{\infty} \psi_n\right]\right)\right) dt - \int\left(\sum_{n=0}^{\infty} \mathbb{A}_n\right) dt,$$

$$\sum_{n=0}^{\infty} \psi_n(x, t) = \mathcal{F}_2(x) + \int \mathcal{G}_2 dt - \int\left(R_2\left(\left[\sum_{n=0}^{\infty} \phi_n\right], \left[\sum_{n=0}^{\infty} \psi_n\right]\right)\right) dt - \int\left(\sum_{n=0}^{\infty} \mathbb{B}_n\right) dt. \tag{10}$$

The following iterative formula is produced by applying the linearity of the integral transform in equation (10)

$$\sum_{n=0}^{\infty}\left[\phi_n(x, t)\right] = \mathcal{F}_1(x) + \int \mathcal{G}_1 dt - \sum_{n=0}^{\infty} \int\left(R_1\left(\phi_n, \psi_n\right)\right) dt - \sum_{n=0}^{\infty} \int \mathbb{A}_n dt,$$

$$\sum_{n=0}^{\infty}\left[\psi_n(x, t)\right] = \mathcal{F}_2(x) + \int \mathcal{G}_2 dt - \sum_{n=0}^{\infty} \int\left(R_2\left(\phi_n, \psi_n\right)\right) dt - \sum_{n=0}^{\infty} \int \mathbb{B}_n dt, \tag{11}$$

Comparing both sides of equation (11) yields the following iterative relation

$$\phi_0 = \mathcal{F}_1(x) + \int \mathcal{G}_1 dt$$

$$\psi_0 = \mathcal{F}_2(x) + \int \mathcal{G}_2 dt \tag{12}$$

For $k \geq 1$, the recursive relation for $(n + 1)$th approximation are given as

$$\phi_{k+1} = -\int R_1(\phi_k,\ \psi_k)\,dt - \int \mathbb{A}_k\,dt,$$

$$\psi_{k+1} = -\int R_2(\phi_k,\ \psi_k)\,dt - \int \mathbb{B}_k\,dt. \tag{13}$$

2.1 *Solution of TWP equation using ADM*

By applying the above-proposed method, we have

$$\phi_0 = H\sqrt{\frac{g}{d}}\,\text{sech}^2\left(\sqrt{\frac{3H}{4d^3}}x\right),$$

$$\psi_0 = H\,\text{sech}^2\left(\sqrt{\frac{3H}{4d^3}}x\right),$$

$$\phi_1 = \left(H\sqrt{\frac{g}{d}}\,\text{sech}^2\left(\sqrt{\frac{3H}{4d^3}}x\right)\right)\left(-2H\sqrt{\frac{3H}{4d^3}}\sqrt{\frac{g}{d}}\,\text{sech}^2\left(\sqrt{\frac{3H}{4d^3}}x\right)\tanh\left(\sqrt{\frac{3H}{4d^3}}x\right)\right)t$$

$$-2gH\sqrt{\frac{3H}{4d^3}}\,\text{sech}^2\left(\sqrt{\frac{3H}{4d^3}}x\right)\tanh\left(\sqrt{\frac{3H}{4d^3}}x\right)t,$$

$$\psi_1 = -2\sqrt{\frac{3H}{4d^3}}H\left(H\sqrt{\frac{g}{d}}\,\text{sech}^2\left(\sqrt{\frac{3H}{4d^3}}\right)\right)\text{sech}^2\left(\sqrt{\frac{3H}{4d^3}}x\right)\tanh\left(\sqrt{\frac{3H}{4d^3}}x\right)t - 2\sqrt{\frac{3H}{4d^3}}H^2\sqrt{\frac{g}{d}}\,\text{sech}^3$$

$$\left(\sqrt{\frac{3H}{4d^3}}x\tanh\left(\sqrt{\frac{3H}{4d^3}}x\right)\right) - 2d\sqrt{\frac{3H}{4d^3}}H\sqrt{\frac{g}{d}}\,\text{sech}^2\left(\sqrt{\frac{3H}{4d^3}}x\right)\tanh\left(\sqrt{\frac{3H}{4d^3}}x\right). \tag{14}$$

So, the approximate solution of the tsunami model is given by

$$\phi(x,t) = H\sqrt{\frac{g}{d}}\,\text{sech}^2\left(\sqrt{\frac{3H}{4d^3}}x\right) + \left(H\sqrt{\frac{g}{d}}\,\text{sech}^2\left(\sqrt{\frac{3H}{4d^3}}x\right)\right)$$

$$\left(-2H\sqrt{\frac{3H}{4d^3}}\sqrt{\frac{g}{d}}\,\text{sech}^2\left(\sqrt{\frac{3H}{4d^3}}x\right)\tanh\left(\sqrt{\frac{3H}{4d^3}}x\right)\right)t$$

$$-2gH\sqrt{\frac{3H}{4d^3}}\,\text{sech}^2\left(\sqrt{\frac{3H}{4d^3}}x\right)\tanh\left(\sqrt{\frac{3H}{4d^3}}x\right)t,$$

$$\psi(x,t) = H\,\text{sech}^2\left(\sqrt{\frac{3H}{4d^3}}x\right) + 2\sqrt{\frac{3H}{4d^3}}H\left(H\sqrt{\frac{g}{d}}\,\text{sech}^2\left(\sqrt{\frac{3H}{4d^3}}\right)\right)\text{sech}^2\left(\sqrt{\frac{3H}{4d^3}}x\right)\tanh\left(\sqrt{\frac{3H}{4d^3}}x\right)t$$

$$-2\sqrt{\frac{3H}{4d^3}}H^2\sqrt{\frac{g}{d}}\operatorname{sech}^3\left(\sqrt{\frac{3H}{4d^3}}x\right)\tanh\left(\sqrt{\frac{3H}{4d^3}}x\right)-2d\sqrt{\frac{3H}{4d^3}}H\sqrt{\frac{g}{d}}\operatorname{sech}^2\left(\sqrt{\frac{3H}{4d^3}}x\right)\tanh\left(\sqrt{\frac{3H}{4d^3}}x\right). \tag{15}$$

3. FDM

3.1 *Discretizing the domain*

We divide the finite temporal domain $[0, T]$ in equidistant mesh points in the following way

$$0 = t_0 < t_1 < t_2 < \ldots < t_n = T$$

and the finite spatial domain $[0, L]$ in the following way

$$0 = x_0 < x_1 < x_2 < \ldots < x_m = L.$$

After this discretization, one can assume that the two-dimensional $x - t$ plane is composed of points (t_i, x_j) where $i = 0, 1, 2, \ldots, n$ and $j = 0, 1, 2, \ldots, m$. We further assume that $x_{i+1} - x_i = \Delta x = h$(say) and $t_{j+1} - t_j = \Delta t$. Under this assumption, the exact values of $\phi(x, t)$ and $\psi(x, t)$ on the grid are approximated by

$$\phi_i^j \approx \phi(ih, j\Delta t), \ \ \psi_i^j \approx \psi(ih, j\Delta t).$$

3.2 *Replacing derivatives by finite difference*

Here, we use the forward time-centered space scheme to approximate the derivative. Using this scheme, one can replace the derivatives $\frac{\partial \phi}{\partial t}$ by $\frac{\phi_i^{j+1} - \phi_i^j}{\Delta t}$ and $\frac{\partial \phi}{\partial x}$ by $\frac{\phi_{i+1}^j - \phi_{i-1}^j}{2h}$ and similarly for the other derivatives $\frac{\partial \psi}{\partial t}$ and $\frac{\partial \psi}{\partial x}$. This explicit numerical scheme requires a stability condition called the Courant condition that gives us an upper bound of the maximum allowable steps for the approximation. The discretized equation takes the form

$$\frac{\phi_i^{j+1} - \phi_i^j}{\Delta t} + \phi_i^j \frac{\phi_{i+1}^j - \phi_{i-1}^j}{2h} + g\frac{\psi_{i+1}^j - \psi_{i-1}^j}{2h} = 0,$$

$$\frac{\psi_i^{j+1} - \psi_i^j}{\Delta t} + d'\frac{\phi_{i+1}^j - \phi_{i-1}^j}{2h} + \phi_i^j \frac{\psi_{i+1}^j - \psi_{i-1}^j}{2h} + \psi_i^j \frac{\phi_{i+1}^j - \phi_{i-1}^j}{2h} = 0$$

with initial conditions

$$\phi_i^0 = \phi(i\Delta x, 0) = H\sqrt{\frac{g}{d}}\operatorname{sech}^2\left(\sqrt{\frac{3H}{4d^3}}i\Delta x\right), \ \ \psi_i^0 = \psi(i\Delta x, 0) = H\operatorname{sech}^2\left(\sqrt{\frac{3H}{4d^3}}i\Delta x\right). \tag{16}$$

4. Solution of TWP equation using FDM

We assume that the solution of the above equation is of the form

$$\phi_i^j = G^j e^{I\beta ih} \text{ and } \psi_i^j = H^j e^{I\gamma ih}$$

where $G = e^{I\alpha_1 \Delta t}$ and $H = e^{I\alpha_2 \Delta t}$ are the growth factors with $-\pi < \alpha_1 < \pi$ and $-\pi < \alpha_2 < \pi$ are the grid wave number and $e^{Ix} = \cos x + I \sin x$. Substituting the values of ϕ_i^j in the first equation of (16), we obtain

$$\frac{G^{j+1} e^{I\beta ih} - G^j e^{I\beta ih}}{\Delta t} + G^j e^{I\beta ih} \frac{G^j e^{I\beta(i+1)h} - G^j e^{I\beta(i-1)h}}{2h} + g \frac{H^j e^{I\gamma(i+1)h} - H^j e^{I\gamma(i-1)h}}{2h} = 0. \tag{17}$$

Simplifying, we get

$$\frac{G-1}{\Delta t} + G^j \frac{e^{I\beta(i+1)h} - e^{I\beta(i-1)h}}{2h} + \frac{gH^j}{G^j e^{I\beta ih}} \frac{e^{I\gamma(i+1)h} - e^{I\gamma(i-1)h}}{2h} = 0,$$

$$\frac{G-1}{\Delta t} + G^j e^{I\beta ih} \frac{e^{I\beta h} - e^{-I\beta h}}{2h} + \frac{gH^j e^{I\gamma zih}}{G^j e^{I\beta ih}} \frac{e^{I\tau h} - e^{-I\gamma h}}{2h} = 0,$$

$$\frac{G-1}{\Delta t} + G^j e^{I\beta ih} \frac{I \sin \beta h}{h} + \frac{gH^j e^{I\gamma ih}}{G^j e^{I\beta ih}} \frac{I \sin \gamma h}{h} = 0. \tag{18}$$

From equation (18), we get

$$\frac{\Delta t}{h} = -\frac{(G-1)G^j}{G^{2j} e^{I\beta ih} I \sin(\beta h) + gH^j e^{I\gamma ih} I \sin(\gamma h)}. \tag{19}$$

Similarly, by substituting ψ_i^j in the second equation of (16), one can have

$$\frac{\Delta t}{h} = -\frac{H^j (H-1)}{d' G^j I \sin(\beta h) + (GH)^j e^{I\gamma ih} I(\sin(\beta h) + \sin(\gamma h))}. \tag{20}$$

Therefore, one can conclude that

$$|\lambda| < \max\{M_1, M_2\}$$

where

$$M_1 = \left| \frac{G^j (G-1)}{G^{2j} e^{I\beta ih} \sin(\beta h) + gH^j e^{I\gamma ih} \sin(\gamma h)} \right|, \; M_2 = \left| \frac{H^j (H-1)}{d' G^j \sin(\beta h) + (GH)^j e^{I\gamma ih} (\sin(\beta h) + \sin(\gamma h))} \right|$$

and $\lambda = \frac{\Delta t}{\Delta x} = \frac{\Delta t}{h}$. Hence, the maximum allowable time step so that the above numerical scheme is stable is given by

$$\Delta t \le 2\Delta x \max\{M_1, \; M_2\}.$$

Since an exact solution is not possible in our model, we evaluate the numerical performance of our scheme, and the rate of convergence can be calculated using the formula [34, 35]

$$S^T = \frac{\ln \frac{F_k}{F_{\frac{k}{2}}}}{\ln(2)},\ W^T = \frac{\ln \frac{L_k}{L_{\frac{k}{2}}}}{\ln(2)}, \tag{21}$$

where $F_k = \|\phi_k - \phi_{2k}\|$, $F_{\frac{k}{2}} = \left\|\phi_{\frac{k}{2}} - \phi_k\right\|$, and $L_k = \|\psi_k - \psi_{2k}\|$, $L_{\frac{k}{2}} = \left\|\psi_{\frac{k}{2}} - \psi_k\right\|$.

5. Results and discussion

Table 1. Comparison of numerical values $\phi(x, t)$ obtained using FDM and ADM method with FRDTM

x	$t = 0$			$t = 1$		
	FDM	ADM	FRDTM	FDM	ADM	FRDTM
00	1.4	1.4	1.4	1.42177	1.4	1.332601
10	1.36287	1.374086129	1.374075	1.45623	1.295392634	1.391195
20	1.28026	1.300077852	1.300035	1.43652	1.154577748	1.399288
30	1.18799	1.188077747	1.187993	1.37977	0.9958547344	1.353778
40	1.05166	1.051790683	1.051662	1.26732	0.8356148664	1.260386
50	0.90514	0.9053023794	0.905137	1.12423	0.6856814176	1.131967
60	0.76036	0.7605531636	0.760364	0.96758	0.5528209456	0.984506
70	0.62585	0.6260541701	0.625855	0.81179	0.4396464913	0.832996
80	0.50656	0.5067570668	0.506559	0.66692	0.3459798996	0.688861
90	0.40446	0.4046490707	0.404461	0.53867	0.2700820093	0.559193
100	0.32721	0.3196211722	0.319449	0.43933	0.2095370897	0.447274
	$t = 2$			$t = 3$		
00	1.31272	1.4	1.130402	1.06287	1.4	0.793404
10	1.43075	1.216699140	1.285101	1.24687	1.138005644	1.055793
20	1.50734	1.009077642	1.405928	1.43028	0.8635775376	1.319957
30	1.51812	0.8036317207	1.466554	1.5372	0.6114087081	1.526321
40	1.46773	0.6194390487	1.454084	1.59747	0.4032632311	1.632759
50	1.35766	0.4660604556	1.373129	1.56838	0.2464394937	1.628621
60	1.20775	0.3450887278	1.241419	1.46276	0.1373565099	1.531106
70	1.03941	0.2532388126	1.081598	1.30361	0.668311337e-1	1.371659
80	0.87055	0.1852027324	0.914236	1.12084	0.0244255652	1.182683
90	0.71339	0.1355149478	0.754299	0.93625	0.0009478864	0.989778
100	0.58758	0.0994530072	0.610634	0.78099	-0.106310754e-1	0.809530

This section examines the acquired methodologies, such as ADM and FDM, utilizing data and graphics. And to validate the outcome, contrast these proposed methods with the fractional reduced differential transform method (FRDTM). The numerical solutions of the TWP model for the tsunami wave's velocity $\phi(x, t)$ and hight $\psi(x, t)$ at various x and t are shown in Tables 1 and 2. Figures 1 and 2 also provide a graphical examination of the TWP model for amplification value $H = 20$ and sea depth $D = 2$. This demonstrates how the tsunami's speed and height remain constant, yet it continues to grow and move quickly. This frequently occurs because no slope allows the wave to break.

Table 2. Comparison of numerical values $\psi(x, t)$ obtained using FDM and ADM method with FRDTM

x	$t = 0$			$t = 1$		
	FDM	ADM	FRDTM	FDM	ADM	FRDTM
00	2	2	2	2.03423	2	1.902245
10	1.96296	1.962980185	1.962964	2.08515	1.957956349	1.996264
20	1.85719	1.857254075	1.857193	2.08219	1.848423053	2.016062
30	1.69713	1.697253924	1.697133	1.99252	1.686513550	1.955509
40	1.50237	1.502558119	1.502374	1.83199	1.491768149	1.822597
50	1.29305	1.293289113	1.293054	1.62505	1.283761182	1.636738
60	1.08623	1.086504519	1.086235	1.39751	1.078859074	1.422243
70	0.89408	0.8943631002	0.894078	1.17107	0.8886638136	1.201767
80	0.72366	0.7239386668	0.723655	0.96075	0.7199269912	0.992348
90	0.5778	0.5780701010	0.577801	0.77492	0.5753699590	0.804385
100	0.45636	0.4566016746	0.456356	0.61669	0.4548465801	0.642547
		$t = 2$			$t = 3$	
00	1.87837	2	1.608980	1.51844	2	1.120205
10	2.02806	1.952932513	1.851124	1.73938	1.947908677	1.527544
20	2.17185	1.839592030	2.041451	2.03239	1.830761008	1.933360
30	2.21063	1.675773176	2.138267	2.24798	1.665032803	2.245405
40	2.14034	1.480978180	2.122279	2.34134	1.470188210	1.632759
50	1.97894	1.274233250	2.002068	2.29856	1.264705319	2.389042
60	1.75751	1.071213629	1.806105	2.13908	1.063568184	2.237820
70	1.50909	0.8829645270	1.569438	1.90235	0.8772652404	1.997092
80	1.26079	0.7159153155	1.323056	1.63071	0.7119036399	1.715780
90	1.03071	0.5726698171	1.088928	1.35803	0.5699696751	1.431429
100	0.82844	0.4530914856	0.879657	1.10608	0.4513363911	1.167686

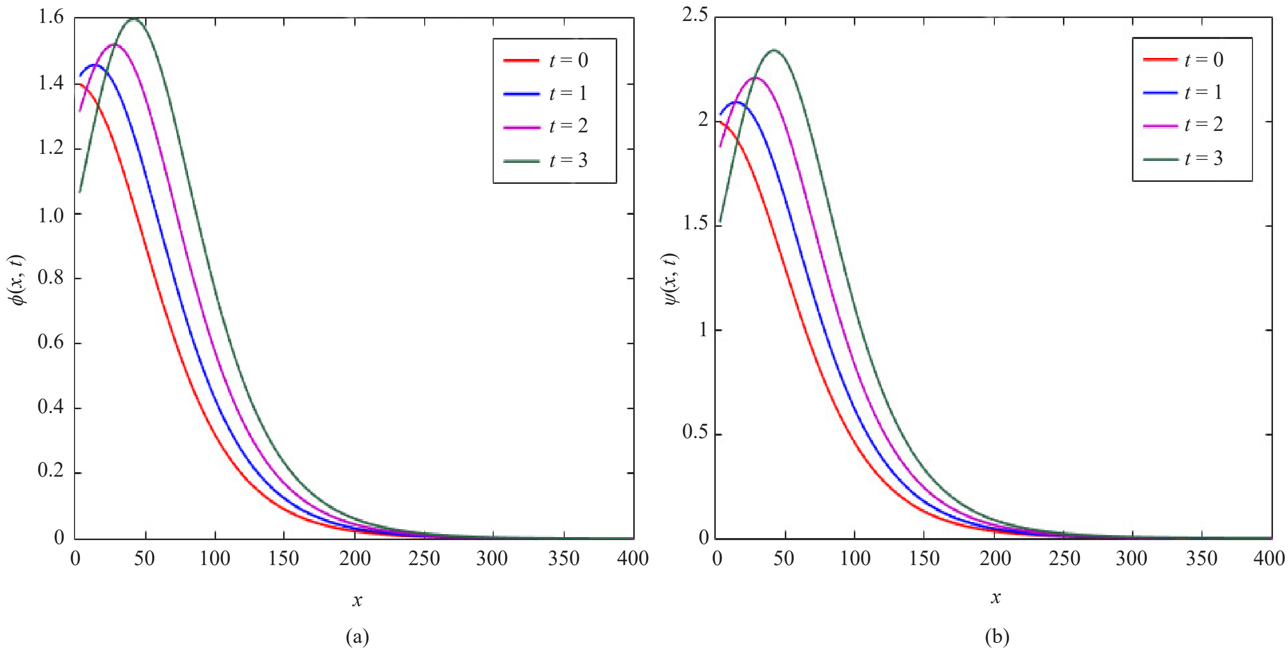

Figure 1. Graph of velocity (ϕ) and height (ψ) for TWP at various time scales

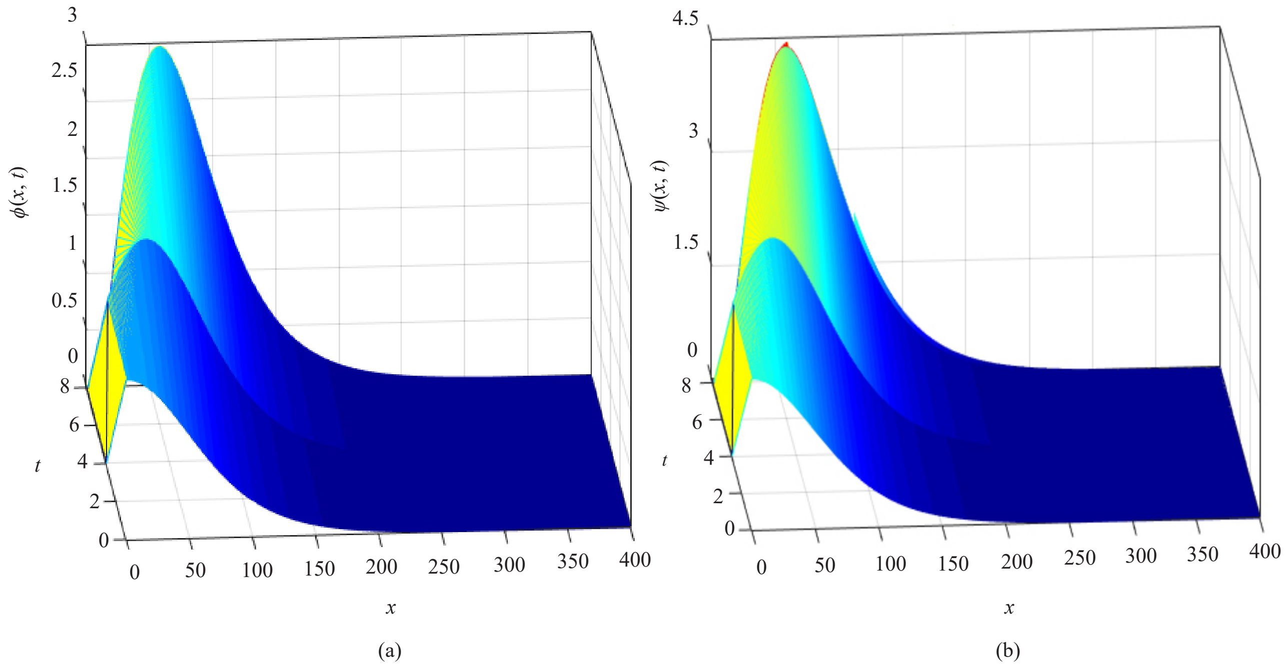

Figure 2. 3D representation of TWP velocity (ϕ) and height (ψ) for various t and x values

Further, we have shown the accuracy of the ADM and FDM in Figure 3 by comparing the obtained numerical values with the FRDTM [19] solutions. It can be said that the error of the ADM technique with respect to the FRDTM is greater than the error of the FDM method with respect to the FRDTM. In contrast to the ADM approach, FDM provides a more precise solution for the TWP model.

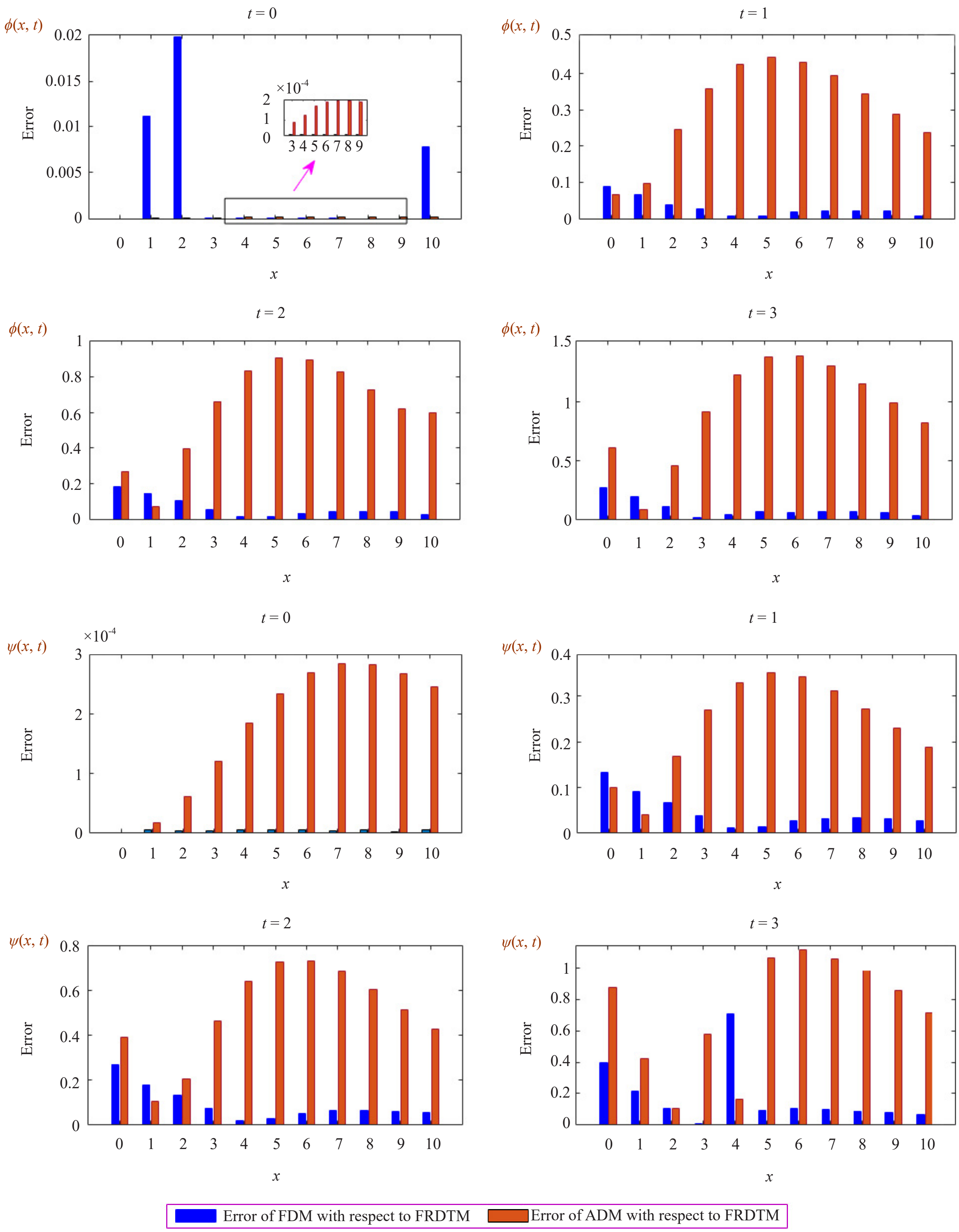

Figure 3. Error analysis of FDM and ADM with respect to FRDTM

6. Conclusions

Here, we have successfully applied ADM and FDM to find the solution of TWP along with its error analysis in the mid-sea and the shore. ADM and FDM give continuous and computationally efficient solutions, providing a more realistic representation of the model. Figure 1 illustrates how the tsunami height and wave velocity preserve their form as they dissipate at a uniform height and velocity. We can conclude that the speed and height of tsunami waves are inversely proportional to the depth of the ocean. When the findings acquired using ADM and FDM approaches are compared with those produced using FRDTM, they are discovered to be in good agreement. The FDM produces the best results when compared to the ADM, according to the error analysis of both approaches with respect to the FRDTM. FDM is, therefore, more appropriate and effective than ADM.

Conflict of interest

There is no conflict of interest in this study.

References

[1] Parwanto NB, Tatsuo O. A statistical analysis and comparison of historical earthquake and tsunami disasters in Japan and Indonesia. *International Journal of Disaster Risk Reduction*. 2014; 7: 122-141. Available from: https://doi.org/10.1016/j.ijdrr.2013.10.003.

[2] Mousa MM. Efficient numerical scheme based on the method of lines for the shallow water equations. *Journal of Ocean Engineering and Science*. 2018; 3(4): 303-309. Available from: https://doi.org/10.1016/j.joes.2018.10.006.

[3] Cecioni C, Bellotti G. Generation and propagation of frequency-dispersive tsunamis. In: Morner N-A. (ed.) *The Tsunami Threat-Research and Technology*. Intech; 2011. Available from: https://doi.org/10.5772/13372.

[4] Tan A, Chilvery AK, Dokhanian M, Crutcher SH. Tsunami propagation models based on first principles. In: Lopez GI. (ed.) *Tsunami-Analysis of a Hazard-From Physical Interpretation to Human Impact*. Intech; 2012. Available from: https://doi.org/10.5772/50508.

[5] Kesarwani J, Meher R. Modelling of an imbibition phenomenon in a heterogeneous cracked porous medium on small inclination. *Special Topics & Reviews in Porous Media: An International Journal*. 2021; 12(1): 27-52. Available from: https://doi.org/10.1615/SpecialTopicsRevPorousMedia.2020030994.

[6] Kesarwani J, Meher R. Numerical study of forced imbibition phenomenon in fluid flow through a water-wet porous media. *International Journal of Computational Materials Science and Engineering*. 2021; 10(3): 2150016. Available from: https://doi.org/10.1142/S2047684121500160.

[7] Kesarwani J, Meher, R. Analytical study of time-fractional porous medium equation using homotopy analysis method. *AIP Conference Proceedings*. 2021; 2336(1): 020004. Available from: https://doi.org/10.1063/5.0046222.

[8] Kesarwani J, Meher, R. Effect of wettability on forced imbibition phenomena in a two-phase flow process through fractured porous media. *Journal of Porous Media*. 2022; 25(1): 41-82. Available from: https://doi.org/10.1615/JPorMedia.2021035092.

[9] Khater MMA. Novel computational simulation of the propagation of pulses in optical fibers regarding the dispersion effect. *International Journal of Modern Physics B*. 2022; 37(9): 2350083. Available from: https://doi.org/10.1142/S0217979223500832.

[10] Khater MMA. A hybrid analytical and numerical analysis of ultra-short pulse phase shifts. *Chaos, Solitons & Fractals*. 2022; 169: 113232. Available from: https://doi.org/10.1016/j.chaos.2023.113232.

[11] Khater MMA, Alfalqi SH, Alzaidi JF, Attia RAM. Analytically and numerically, dispersive, weakly nonlinear wave packets are presented in a quasi-monochromatic medium. *Results in Physics*. 2023; 46: 106312. Available from: https://doi.org/10.1016/j.rinp.2023.106312.

[12] Khater MMA. Prorogation of waves in shallow water through unidirectional Dullin-Gottwald-Holm model; computational simulations. *International Journal of Modern Physics B*. 2023; 37(8): 2350071. Available from: https://doi.org/10.1142/S0217979223500716.

[13] Khater MMA. In solid physics equations, accurate and novel soliton wave structures for heating a single crystal of sodium fluoride. *International Journal of Modern Physics B*. 2023; 37(7): 2350068. Available from: https://doi.

org/10.1142/S0217979223500686.
[14] Khater MMA. Nonlinear elastic circular rod with lateral inertia and finite radius: Dynamical attributive of longitudinal oscillation. *International Journal of Modern Physics B*. 2023; 37(6): 2350052. Available from: https://doi.org/10.1142/S0217979223500522.
[15] Khater MMA, Zhang X, Attia RAM. Accurate computational simulations of perturbed Chen-Lee-Liu equation. *Results in Physics*. 2023; 45: 106227. Available from: https://doi.org/10.1016/j.rinp.2023.106227.
[16] Khater MMA. Multi-vector with nonlocal and non-singular kernel ultrashort optical solitons pulses waves in birefringent fibers. *Chaos, Solitons & Fractals*. 2023; 167: 113098. Available from: https://doi.org/10.1016/j.chaos.2022.113098.
[17] Khater MMA. Physics of crystal lattices and plasma; analytical and numerical simulations of the Gilson-Pickering equation. *Results in Physics*. 2023; 44: 106193. Available from: https://doi.org/10.1016/j.rinp.2022.106193.
[18] Attia RAM, Zhang X, Khater MMA. Analytical and hybrid numerical simulations for the (2+1)-dimensional Heisenberg ferromagnetic spin chain. *Results in Physics*. 2022; 43: 106045. Available from: https://doi.org/10.1016/j.rinp.2022.106045.
[19] Tandel P, Patel H, Patel T. Tsunami wave propagation model: A fractional approach. *Journal of Ocean Engineering and Science*. 2022; 7(6): 509-520. Available from: https://doi.org/10.1016/j.joes.2021.10.004.
[20] Chaturvedi SK, Guven U, Srivastava PK. Measurement and validation of tsunami Eigen values for the various water wave conditions. *Journal of Ocean Engineering and Science*. 2020; 5(1): 41-54. Available from: https://doi.org/10.1016/j.joes.2019.08.001.
[21] Alotaibi MF, Omri M, Khalil EM, Abdel-Khalek S, Bouslimi J, Khater MMA. Abundant solitary and semi-analytical wave solutions of nonlinear shallow water wave regime model. *Journal of Ocean Engineering and Science*. 2022. Available from: https://doi.org/10.1016/j.joes.2022.02.005.
[22] Synolakis CE, Bernard EN, Titov VV, Kânoğlu U, González FI. Validation and verification of tsunami numerical models. *Pure and Applied Geophysics*. 2008; 165: 2197-2228. Available from: https://doi.org/10.1007/s00024-004-0427-y.
[23] Majumder A, Adak D, Bairagi N. Persistence and extinction of species in a disease-induced ecological system under environmental stochasticity. *Physical Review E*. 2021; 103(3): 032412. Available from: https://doi.org/10.1103/PhysRevE.103.032412.
[24] Majumder A, Adak D, Bairagi N. Phytoplankton-zooplankton interaction under environmental stochasticity: Survival, extinction and stability. *Applied Mathematical Modelling*. 2021; 89: 1382-1404. Available from: https://doi.org/10.1016/j.apm.2020.06.076.
[25] Meher R, Kesarwani J, Avazzadeh Z, Nikan O. Numerical treatment of temporal-fractional porous medium model occurring in fractured media. *Journal of Ocean Engineering and Science*. 2022; 8(5): 481-499. Available from: https://doi.org/10.1016/j.joes.2022.02.016.
[26] Kesarwani J, Meher R. Computational study of time-fractional porous medium equation arising in fluid flow through a water-wet porous media. *International Journal of Computational Materials Science and Engineering*. 2020; 9(2): 2050007. Available from: https://doi.org/10.1142/S2047684120500074.
[27] Kesarwani J, Meher R. Mathematical modelling of fingering phenomenon using homotopy analysis method. *AIP Conference Proceedings*. 2020; 2214(1): 020029. Available from: https://doi.org/10.1063/5.0003558.
[28] Regina MY, Mohamed ES. Study on analytical modelling of tsunami wave propagation. *Intelligent Systems and Computer Technology*. 2020; 37: 479-484. Available from: https://doi.org/10.3233/APC200188.
[29] Younesian D, Askari H, Saadatnia Z, Yıldırım A. Analytical solution for nonlinear wave propagation in shallow media using the variational iteration method. *Waves in Random and Complex Media*. 2012; 22(2): 133-142. Available from: https://doi.org/10.1080/17455030.2011.633578.
[30] Karunakar P, Chakraverty S. Homotopy perturbation method for predicting tsunami wave propagation with crisp and uncertain parameters. *International Journal of Numerical Methods for Heat & Fluid Flow*. 2021; 31(1): 92-105. Available from: https://doi.org/10.1108/HFF-11-2019-0861.
[31] Baskonus HM, Eskitascioglu EI. Complex wave surfaces to the extended shallow water wave model with (2+1)-dimensional. *Computational Methods for Differential Equations*. 2020; 8(3): 585-596. Available from: https://doi.org/10.22034/cmde.2020.31374.1471.
[32] Yel G, Baskonus HM, Gao W. New dark-bright soliton in the shallow water wave model. *AIMS Mathematics*. 2020; 5(4): 4027-4044. Available from: https://doi.org/10.3934/math.2020259.
[33] Adomian G. *Solving Frontier Problems of Physics: The Decomposition Method*. Dordrecht: Springer; 1994. Available from: https://doi.org/10.1007/978-94-015-8289-6.
[34] Bhatt HP, Khaliq AQM. Fourth-order compact schemes for the numerical simulation of coupled Burgers'

equation. *Computer Physics Communications*. 2016; 200: 117-138. Available from: https://doi.org/10.1016/j.cpc.2015.11.007.

[35] Tijani YO, Appadu AR, Aderogba AA. Some finite difference methods to model biofilm growth and decay: Classical and non-standard. *Computation*. 2021; 9(11): 123. Available from: https://doi.org/10.3390/computation9110123.